Supplemental material

Potenza et al., https://doi.org/10.1085/jgp.201812155

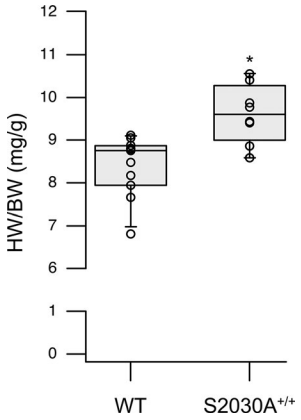

Figure S1. **S2030A$^{+/+}$ display a higher HW/BW ratio compared with WT animals.** HW/BW ratio was measured and used as an index of hypertrophy (see Materials and methods for details; WT: N = 11; 31.25 ± 1.07 g [BW]; 262 ± 8 mg [HW]; 8.41 ± 0.21 [HW/BW]; S2030A$^{+/+}$: *N* = 8; 32.45 ± 0.86 g [BW]; 311 ± 9 mg [HW]; 9.61 ± 0.24 [HW/BW]). The data are expressed as mean ± SEM of all measurements. *, P < 0.05 versus WT. The whiskers cover the range from 10% to 90%.

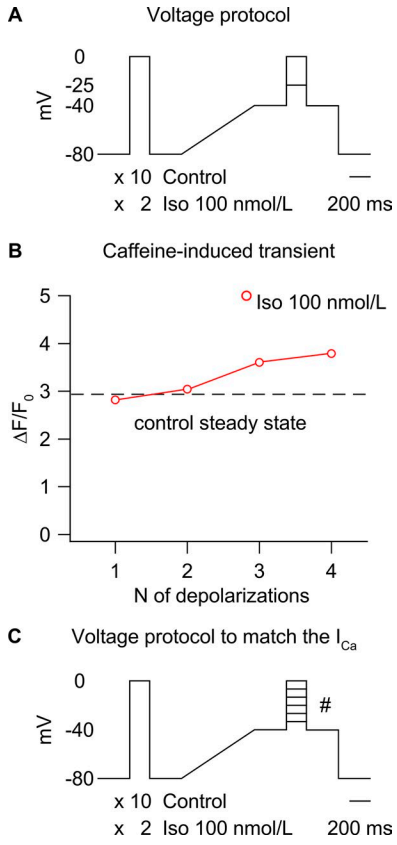

Figure S2. **Recording protocols. (A)** Myocytes were held at a potential of −80 mV, and an initial step to −40 mV was applied to inactivate Na^+ and T-type Ca^{2+} currents. For each cell, peak Ca^{2+} current was then measured at two membrane potentials (from −40 to −25 mV and −40 to 0 mV) in control and during subsequent Iso application. The extent of SR Ca^{2+} loading in a single cell was controlled under whole-cell patch-clamp conditions by using a train with a different number of depolarization steps (10 for control and 2 for Iso) of 200-ms duration at 0.5 Hz. **(B)** The train of depolarizations was preceded by a rapid caffeine exposure in order to reset SR Ca^{2+} content, and the steady-state in control was achieved after 10 depolarization steps. In Iso, after the initial caffeine application, the SR was reloaded with one, two, three, and four depolarizations. We estimated the SR Ca^{2+} content from the peak amplitude of the caffeine-induced transient ($\Delta F/F_0$), and we compared control steady state and Iso at an increasing number of stimulations. The amplitude after two depolarizations in Iso was the closest value to control, and it was used to match the control SR Ca^{2+} content. A cell was considered for analysis when the difference between control and Iso SR Ca^{2+} load was within ±15% (>75% of the patched myocytes). The cells that did not meet the criteria were excluded. **(C)** To compare the ECC gain in myocytes with similar SR Ca^{2+} load and similar I_{Ca}, additional recordings were performed for both WT and S2030A$^{+/+}$ animals. Starting from the same loading protocol shown in A, the cells were selected according to their SR Ca^{2+} content (mean WT ±15%). For these measurements, the I_{Ca} trigger was also maintained constant between groups using a recording protocol with variously sized I_{Ca}. After the conditioning step, six currents (#) were recorded, from −40 to −25 mV up to 0 mV (+5-mV steps) in control and from −40 to −35 mV up to −10 mV for Iso. In Iso, an extra recording was performed with a different range of I_{Ca} trigger (from −40 to −30 mV up to −15 mV, with +3-mV steps). Between the recorded currents, a matching pair was selected per each cell (WT and mutant) considering the mean WT I_{Ca} (±15%). A cell was considered for analysis when the difference between the I_{Ca} in control and Iso was within ±15%. The cells that did not meet the criteria were excluded.

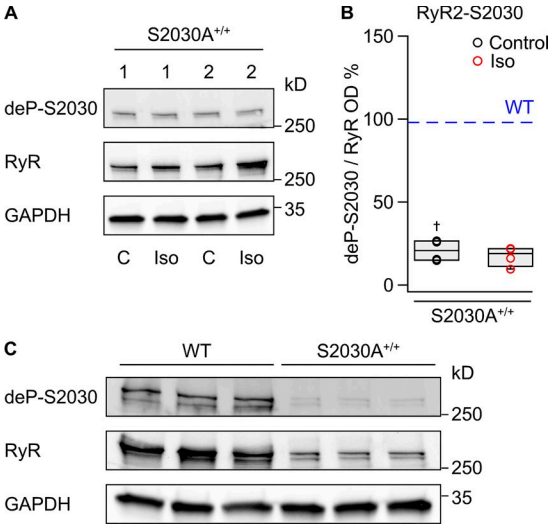

Figure S3. **Iso treatment does not change the dephospho-RyR2-S2030/RyR fraction in RyR2-S2030A$^{+/+}$ cells. (A)** Representative Western blot showing the signal generated by the dephospho-RyR2-S2030 Ab in myocytes isolated from S2030A$^{+/+}$ animals (N = 4) before (C, control) and after application of 100 nmol/liter Iso. The numbers 1 and 2 identify different animals. Numbers on the right (250 and 35 kDa) refer to the protein ladder. **(B)** The dephospho-RyR2-S2030/RyR ratio was significantly lower compared with WT. The dashed blue line represents the median of the WT dephospho-RyR2-S2030/RyR fraction reported in Fig. 2. In contrast to WT, the signal was not modified by Iso confirming, indirectly, the ablation of the phosphorylation site. The level of the phosphorylation was expressed as ratio of the dephospho-RyR2-S2030 and the anti-RyR Ab OD, both normalized to the GAPDH signal. There are two possible reasons for the low signal detected by the dephospho-Ab in S2030A$^{+/+}$ cells: (1) there is less RyR2 expression in S2030A$^{+/+}$ cells, and (2) the dephospho-Ab (designed to recognize the dephospho-S2030 site in WT) weakly binds the epitope with the alanine substitution (S2030A$^{+/+}$), which suggests specificity of the dephospho-Ab for the S2030 site. **(C)** Blot showing comparison between WT and S2030A$^{+/+}$ cells. †, $P < 0.05$ S2030A$^{+/+}$ versus WT. The whiskers cover the range from 10% to 90%.

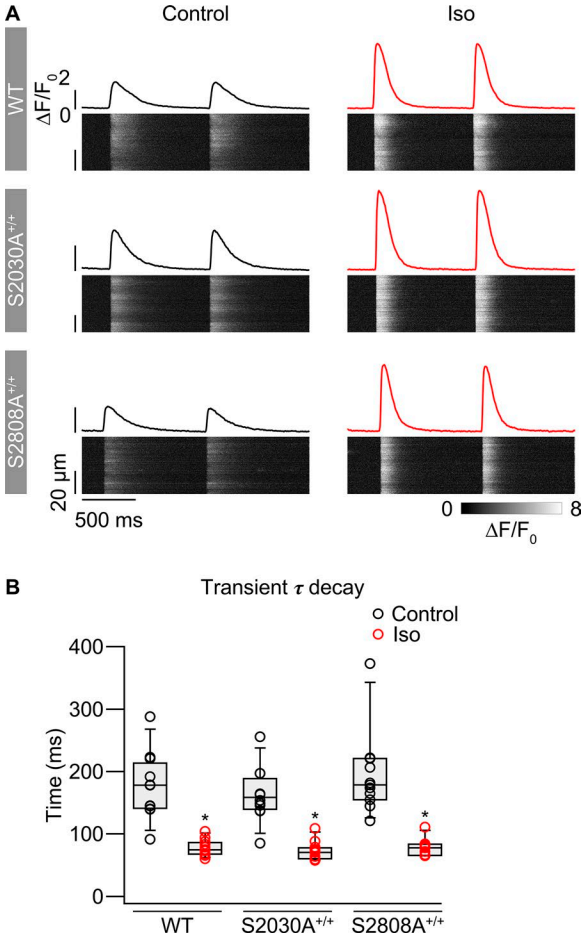

Figure S4. **Acceleration of the time course of the Ca^{2+} transient decay by Iso.** The cells were electrically stimulated at 1 Hz for 30 s. **(A)** Representative line profiles of the Ca^{2+} transients as relative changes in cytosolic Ca^{2+} concentrations ($\Delta F/F_0$; black traces for the control and red for Iso) and the corresponding confocal line-scan images for WT, S2030A$^{+/+}$, and S2808A$^{+/+}$ fluo-3 AM–loaded myocytes. **(B)** τ decay of Ca^{2+} transients before and after Iso application for WT (N = 4, *n* = 12), S2030A$^{+/+}$ (N = 4, *n* = 13), and S2808A$^{+/+}$ (N = 3, *n* = 10) myocytes. The amplitude of the Ca^{2+} transients in control and Iso were comparable between the animals (Bers and Berlin, 1995). *, P < 0.05 versus control. The whiskers cover the range from 10% to 90%.

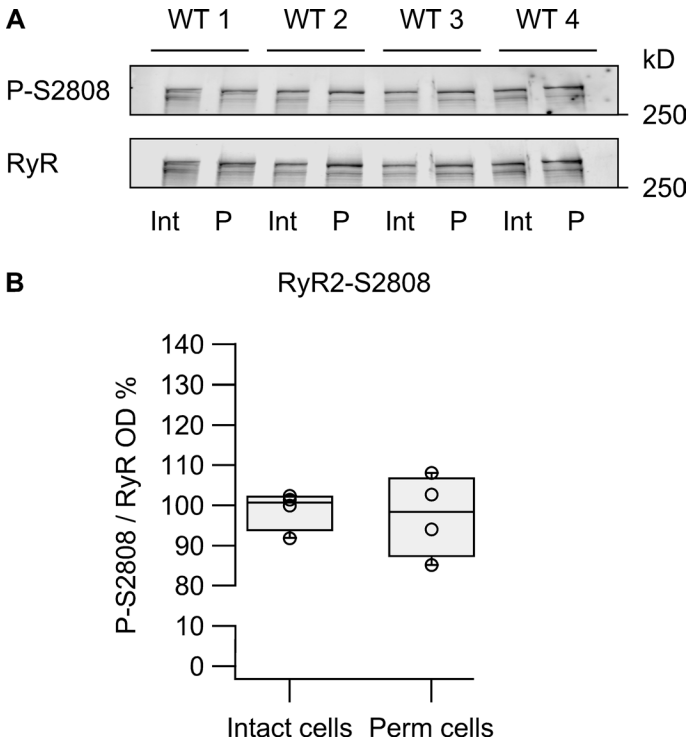

Figure S5. **β-escin permeabilization does not change phosphorylation at the RyR2-S2808 site. (A)** Western blot showing the level of RyR2-S2808 site phosphorylation before (intact cells [Int]) and after (permeabilized cells [P]) 20 min from the cells' permeabilization with β-escin. In the gel, samples from four different WT animals were run simultaneously. The 250 (kDa) label indicates the molecular weight of the protein ladder. **(B)** The level of phosphorylation was expressed as ratio of the anti-phospho-RyR2-S2808 and the total-RyR signals (OD). *, $P < 0.05$ versus intact cells. The whiskers cover the range from 10% to 90%.

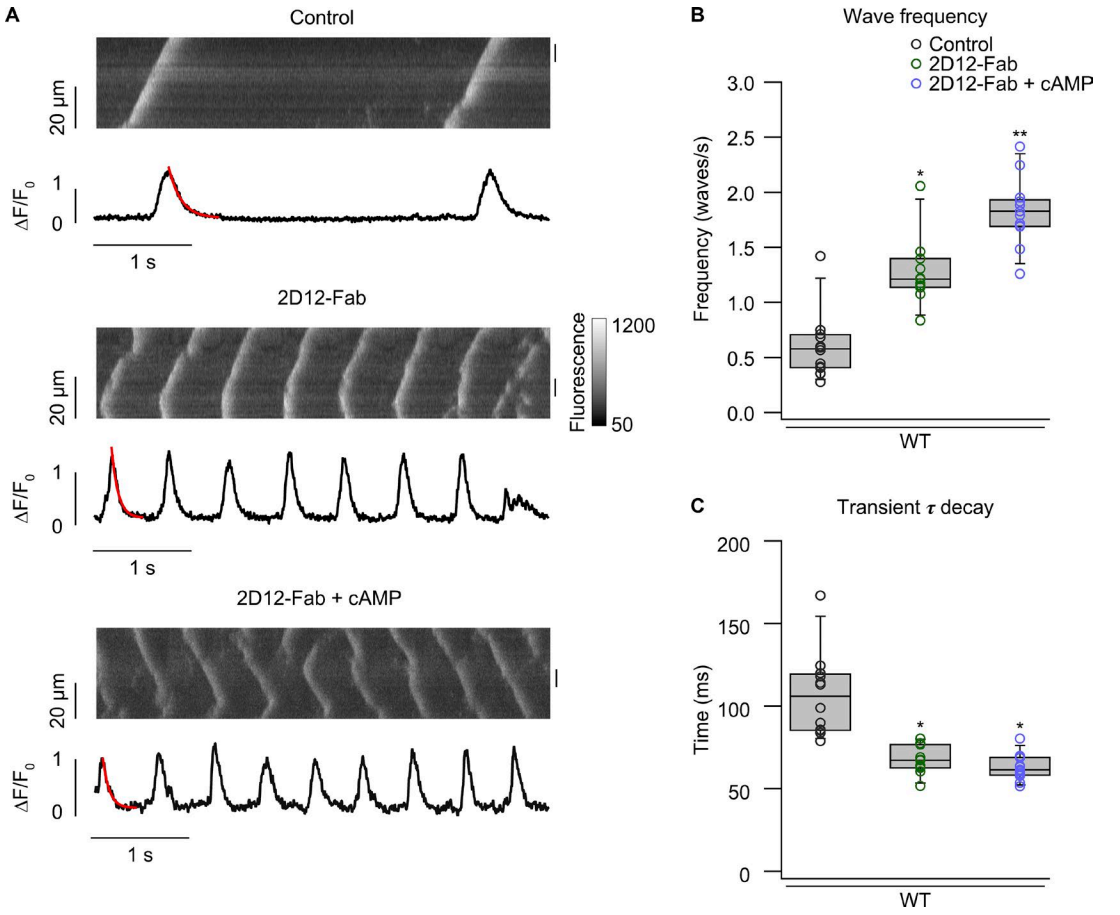

Figure S6. **cAMP does not further accelerate SERCA activity in 2D12-Fab–treated cells. (A)** Representative line scans and line profiles recorded in permeabilized cells before and after treatment with 100 µg/ml 2D12-Fab (15 min) and 20 µmol/liter cAMP. A monoexponential function was used to fit (red lines) the decreasing phase of the Ca^{2+} waves and measure the τ decay, reflecting SR Ca^{2+} pump activity. **(B)** Application of the 2D12-Fab fragment increased the frequency of Ca^{2+} release events. The frequency was further increased after cAMP application (5 min). **(C)** The τ decay was significantly faster in cells treated with the antibody (N = 3, *n* = 11) than in untreated cells (N = 3, *n* = 12), indicating a faster activity of the SERCA pump. Further cAMP application (N = 3, *n* = 14) did not accelerate the decay, suggesting an already fully activated SERCA. *, P < 0.05 versus control; **, P < 0.05 versus 2D12-Fab. The whiskers cover the range from 10% to 90%.

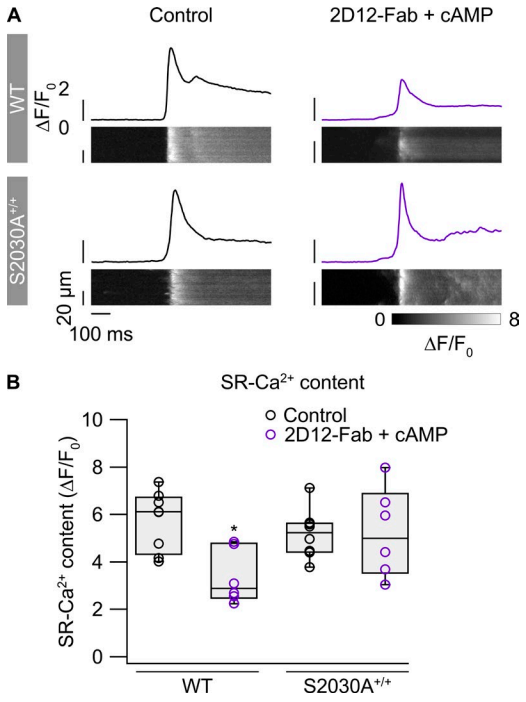

Figure S7. **cAMP decreases SR Ca^{2+} content in 2D12-Fab–treated WT cells. (A)** Representative line-scan images and line profiles of 20 mmol/liter caffeine-dependent Ca^{2+} transients recorded in control and after 2D12-Fab/cAMP combined treatment. **(B)** SR Ca^{2+} content is estimated from the amplitude of the caffeine-transient (expressed as $\Delta F/F_0$). After treatment with the 2D12-Fab fragment, cAMP reduced SR Ca^{2+} content in WT cells, but not in S2030A$^{+/+}$ cells, mirroring the observation of cAMP-induced Ca^{2+} sparks exclusively in WT cells (see Fig. 4; N = 3, *n* = 8 for control and *n* = 6 for 2D12-Fab + cAMP for both animals). *, P < 0.05 versus control. The whiskers cover the range from 10% to 90%.

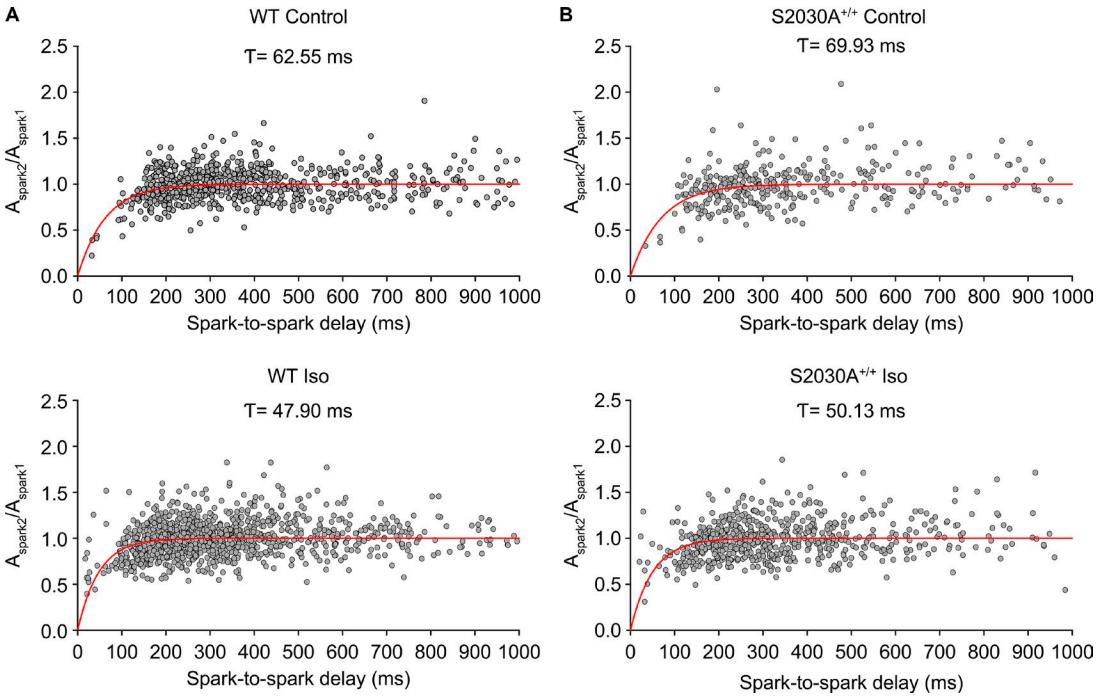

Figure S8. **Spark amplitude restitution. (A and B)** Spark amplitude restitution for WT (A) and S2030A$^{+/+}$ (B) myocytes at control conditions and during β-adrenergic stimulation with 100 nmol/liter Iso. Each plot shows the normalized amplitude of the second spark (A_{spark2}/A_{spark1}) versus the delay between sparks. Spark amplitude ratios were fitted with a single exponential curve (red line; control WT: 62.55 ms, 95% CI, 54.24–70.85 ms, N = 10, *n* = 35, 749 spark pairs; Iso WT: 47.90 ms, 95% CI, 41.65–54.14 ms, N = 11, *n* = 43, 1,196 spark pairs; control S2030A$^{+/+}$: 69.93 ms, 95% CI, 57.59–82.26 ms, N = 6, *n* = 20, 380 spark pairs; Iso S2030A$^{+/+}$: 50.13 ms, 95% CI, 41.38–58.87 ms, N = 7, *n* = 27, 689 spark pairs).

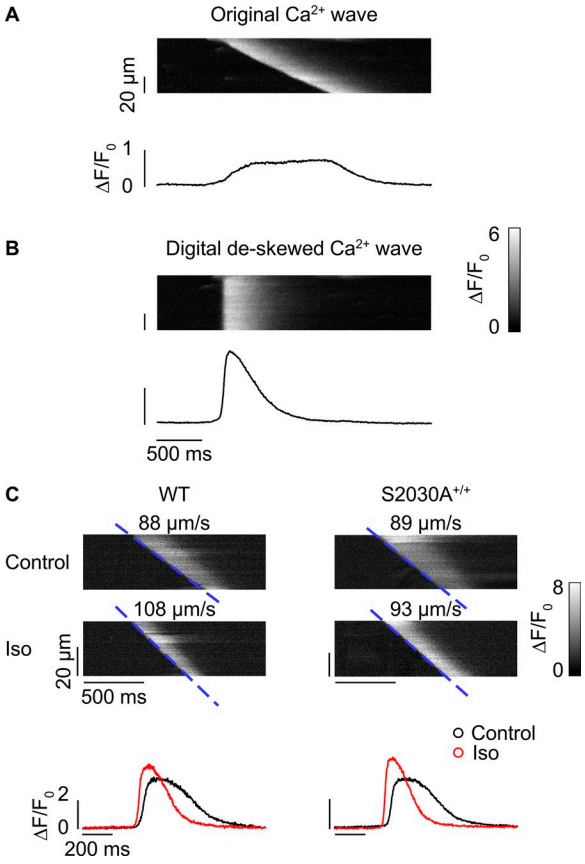

Figure S9. **Ca^{2+} wave analysis.** To evoke the waves, we elevated the extracellular Ca^{2+} concentration to 10 mmol/liter, which resulted in SR Ca^{2+} overload. **(A)** Representative line-scan image and the corresponding line profile of a Ca^{2+} wave induced by high $[Ca^{2+}]_o$. The global line profile did not allow an accurate measurement of the time course of the Ca^{2+} signal. **(B)** The Ca^{2+} wavefront has been aligned by digital deskewing, and the related line profile was used to measure the τ decay of the Ca^{2+} signal (representative of SERCA pump activity). **(C)** Representative line-scan images and line profiles of Ca^{2+} waves measured in WT and S2030A$^{+/+}$ myocytes. The profiles clearly show that SERCA is stimulated by Iso in both cell types (red traces display a faster decreasing phase). Note the differences in the angle of the wavefront (indicated by the blue dashed lines) between WT and S2030A$^{+/+}$ during Iso treatment.

Table S1. **Statistical summary of the echocardiograph measurements**

	Fractional shortening (%)	LV volume diastole (µl)	LV volume systole (µl)	LV B-mode LV ejection fraction (µl)	LV B-mode LV volume (µl)	LV B-mode stroke volume (µl)
WT (N = 7)	31.9 ± 2.0	62.2 ± 4.1	22.3 ± 1.8	57.4 ± 1.4	41.2 ± 2.5	28.2 ± 0.5
S2030A (N = 7)	36.1 ± 4.3	74.4 ± 6	29.0 ± 7	62.9 ± 5.8	42.5 ± 3.5	31.3 ± 2.3

Mice at the age of 3 mo were anesthetized with 5% isoflurane inhalation and maintained in the anesthetized state by 1.5–2% isoflurane. Two-dimensionally guided B-mode imaging was used to measure the LV volume during systole and diastole, the stroke volume, and the ejection fraction. The fractional shortening was also calculated using the formula: [(LV diameter diastole − LV diameter systole)/LV diameter diastole] × 100. The LV diastolic and systolic volume and the fractional shortening and ejection fraction were slightly increased in S2030A$^{+/+}$ animals compared to WT animals, but none of the observed differences was statistically significant (all $P > 0.05$).

Table S2. **Statistical summary of the Ca^{2+} transient amplitude at matched I_{Ca} and SR Ca^{2+} load**

	Matched I_{Ca}	Measured transient amplitude	Matched SR Ca^{2+} content
	(pA/pF)	($\Delta F/F_0$)	($\Delta F/F_0$)
WT (N = 3/*n* = 8)			
Control	2.75 ± 0.07	2.27 ± 0.25	2.80 ± 0.11
Iso	2.80 ± 0.12	2.15 ± 0.18	2.88 ± 0.06
S2030A (N = 4/*n* = 6)			
Control	3.09 ± 0.15	2.13 ± 0.29	2.72 ± 0.09
Iso	3.05 ± 0.12	0.90 ± 0.16[a,b]	2.71 ± 0.14

Using the protocol described in Fig. S2, the SR Ca^{2+} content (measured as the amplitude of the caffeine-evoked transients) was experimentally matched between control and Iso in all cells. We reported a difference in the SR Ca^{2+} load between WT and mutant myocytes (Fig. 1). To further compare WT and S2030A$^{+/+}$ cells, we assessed the ECC gain in conditions of matched SR Ca^{2+} load and matched I_{Ca} between all the groups (see Fig. S2 for details). In these experimental conditions, the Ca^{2+} release in WT myocytes did not change during Iso. However, the Ca^{2+} release was decreased in S2030A$^{+/+}$ after Iso application, corroborating the conclusion that the S2030 site may be involved in RyR2 sensitization during the β-adrenergic response. Data are expressed as means ± SEM of *n* measurements.
[a]P < 0.05 versus control.
[b]P < 0.05 versus WT.

Table S3. **Statistical summary of the Ca^{2+} spark parameters**

	Frequency	Amplitude	FWHM	FDHM	Spark mass
	(sparks/100 µm/s)	($\Delta F/F_0$)	(µm)	(ms)	($\Delta F/F_0 \times \mu m^3$)
WT (N = 4/*n* = 12)					
Control	0.32 ± 0.08	1.10 ± 0.15	2.11 ± 0.12	36.75 ± 2.99	14.51 ± 2.32
Iso	1.95 ± 0.29[a]	1.59 ± 0.15[a]	2.18 ± 0.12	36.59 ± 2.83	38.97 ± 13.19[a]
S2030A (N = 4/*n* = 13)					
Control	0.37 ± 0.07	1.01 ± 0.08	2.09 ± 0.19	36.81 ± 3.49	14.48 ± 4.68
Iso	1.05 ± 0.15[a,b]	1.08 ± 0.09[b]	1.97 ± 0.16	38.03 ± 2.52	15.51 ± 3.49[b]
S2808A (N = 3/*n* = 10)					
Control	0.33 ± 0.07	0.98 ± 0.16	2.14 ± 0.11	39.97 ± 7.46	12.72 ± 1.87
Iso	2.14 ± 0.33[a]	1.28 ± 0.18[a]	2.23 ± 0.18	42.43 ± 3.95	34.13 ± 11.36[a]

Spontaneous Ca^{2+} sparks were recorded in intact cells after a train of electrical stimulations at 1 Hz for 30 s (0.5-ms pulses at 20–40 V) and were quantified with the ImageJ plug-in SparkMaster. Spark mass was calculated as 1.206 × amplitude × FWHM^3. Data are expressed as means ± SEM of *n* measurements. FDHM, full duration at half maximum; FWHM, full width at half maximum.
[a]P < 0.05 versus control.
[b]P < 0.05 versus WT.

References

Bers, D.M., and J.R. Berlin. 1995. Kinetics of $[Ca]_i$ decline in cardiac myocytes depend on peak $[Ca]_i$. *Am. J. Physiol.* 268:C271–C277. https://doi.org/10.1152/ajpcell.1995.268.1.C271